Journal of Materials Chemistry B

Materials for biology and medicine

rsc.li/materials-b

ROYAL SOCIETY OF CHEMISTRY
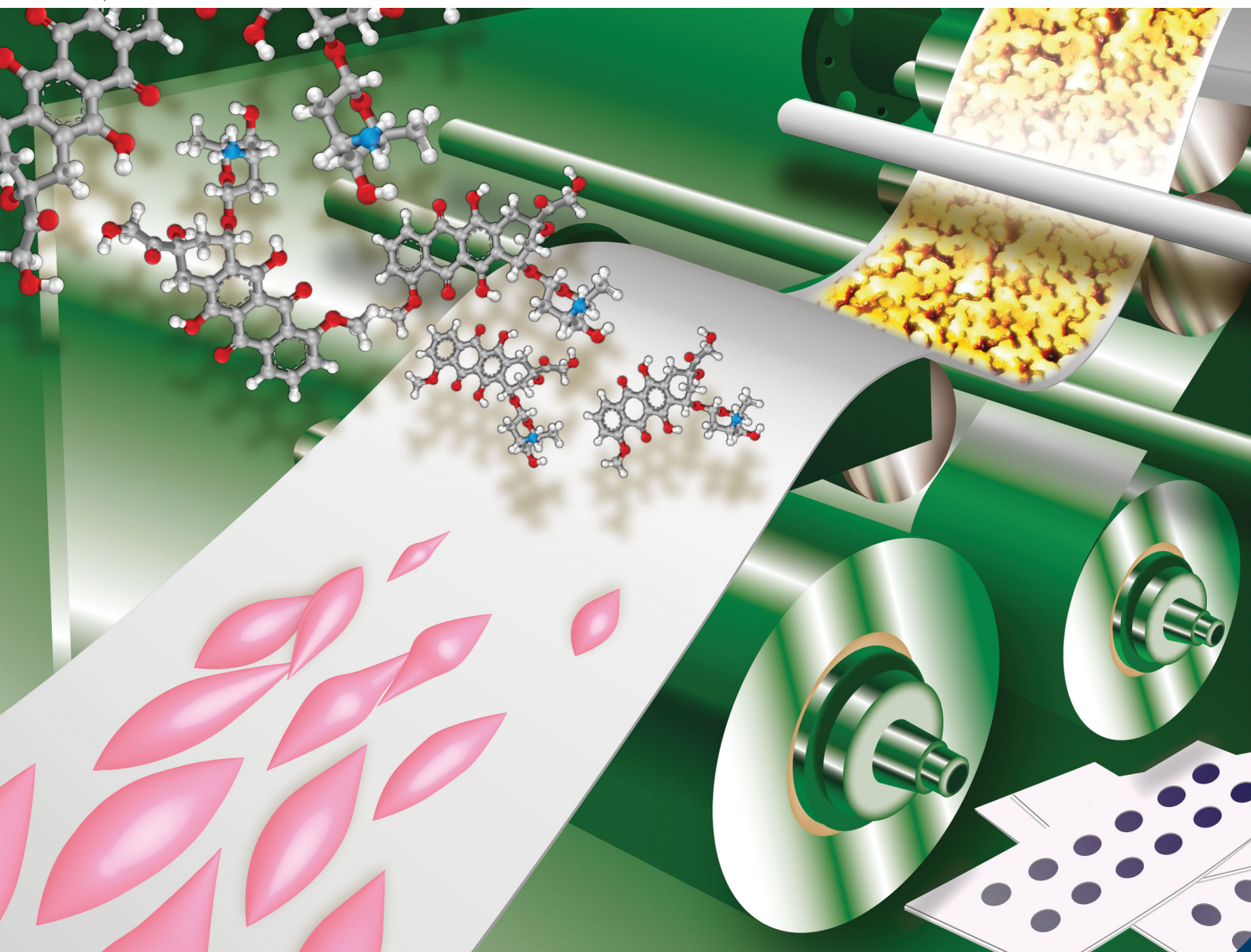
PAPER
E. Rosqvist *et al.*
A low-cost paper-based platform for fast and reliable
screening of cellular interactions with materials

Indexed in Medline!

ROYAL SOCIETY
OF CHEMISTRY

PAPER

Check for updates

A low-cost paper-based platform for fast and reliable screening of cellular interactions with materials†

E. Rosqvist, [ID] ‡*[a] E. Niemelä,‡[bc] J. Frisk,[d] H. Öblom,[e] R. Koppolu, [ID][f]
H. Abdelkader,[bc] D. Soto Véliz,[f] M. Mennillo,[g] A. P. Venu,[bc] P. Ihalainen,[a] M. Aubert,[g]
N. Sandler,[e] C.-E. Wilén,[g] M. Toivakka, [ID][f] J. E. Eriksson,[bc] R. Österbacka[d] and
J. Peltonen[a]

A paper-based platform was developed and tested for studies on basic cell culture, material biocompatibility, and activity of pharmaceuticals in order to provide a reliable, robust and low-cost cell study platform. It is based upon a paper or paperboard support, with a nanostructured latex coating to provide an enhanced cell growth and sufficient barrier properties. Wetting is limited to regions of interest using a flexographically printed hydrophobic polydimethylsiloxane layer with circular non-print areas. The nanostructured coating can be substituted for another coating of interest, or the regions of interest functionalized with a material to be studied. The platform is fully up-scalable, being produced with roll-to-roll rod coating, flexographic and inkjet printing methods. Results show that the platform efficiency is comparable to multi-well plates in colorimetric assays in three separate studies: a cell culture study, a biocompatibility study, and a drug screening study. The color intensity is quantified by using a common office scanner or an imaging device and the data is analyzed by a custom computer software without the need for expensive screening or analysis equipment.

1. Introduction

Currently, *in vitro* cell culture studies are mainly performed on flat transparent plastic polystyrene-based cell culture materials.[1] Optical analysis performed on these plastic well plates, *e.g.* cell growth, invasion assays and protein binding, is commonly conducted using expensive high-resolution microscopes and high-throughput microplate readers, which limits their availability in

[a] *Laboratory of Physical Chemistry, Center for Functional Materials, Åbo Akademi University, Porthansgatan 3-5, 20500 Åbo, Finland. E-mail: emil.rosqvist@abo.fi*
[b] *Laboratory of Cell Biology, Center for Functional Materials, Åbo Akademi University, Bio City, Artillerigatan 6B, 20521 Åbo, Finland*
[c] *Turku Bioscience Centre, University of Turku and Åbo Akademi University, 20520 Åbo, Finland*
[d] *Laboratory of Physics, Center for Functional Materials, Åbo Akademi University, Porthansgatan 3-5, 20500 Åbo, Finland*
[e] *Pharmaceutical Sciences Laboratory, Åbo Akademi University, Artillerigatan 6A, 20520 Åbo, Finland*
[f] *Laboratory of Paper Coating, Center for Functional Materials, Åbo Akademi University, Porthansgatan 3-5, 20500 Åbo, Finland*
[g] *Laboratory of Polymer Technology, Center for Functional Materials, Åbo Akademi University, Biskopsgatan 3-5, 20500 Åbo, Finland*
† Electronic supplementary information (ESI) available. See DOI: 10.1039/c9tb01958h
‡ These authors contributed equally to this work.

regions with limited resources and undeveloped infrastructures.[2,3] Additionally, plastic well plates take up a lot of space during storage and transport, and are non-biodegradable.[4–6] Furthermore, living tissues typically involve soft materials with stiffness between 0.5 kPa and 100 kPa.[7] Hard substrate materials frequently used in cell culture have stiffnesses in the GPa range and do not provide an ideal interface for cells.[4,5,8] This may create a situation where the cells need to introduce stress fibers and increase cell anchoring proteins in order to adhere to these artificial surfaces.[4,5,8] Screening platforms based on softer materials would provide a more realistic environment in which to study cell fate and drug screening, as well as conduct personalized disease treatment.[2,9]

Low-cost point-of-care is essential to prevent and treat diseases to improve the health of the people in developing regions.[10] Contemporary treatments often rely on expensive diagnostic instruments that are unavailable to many – not only in terms of affordability, but also in terms of trained staff. For instance, in Africa the existing infrastructure does not support routine use of laboratory tests, with as few as 26% of technical staff professionally qualified in local hospitals.[11,12] Due to these limitations, misdiagnosis, deficient disease-mapping and inadequate treatments and medication, are common problems.[11] Easy-to-use diagnostic tools would improve the

1146 | *J. Mater. Chem. B*, 2020, **8**, 1146–1156

This journal is © The Royal Society of Chemistry 2020

situation markedly. Indeed, the World Health Organization (WHO) has declared that ideally diagnostic devices should be affordable, sensitive, specific, user-friendly, rapid and robust, equipment-free and deliverable (ASSURED). Nowadays, smartphones are portable pocket-sized computers readily available even in developing countries and are a potential tool for medical analyses.[13] An easily read paper-based diagnostic platform would fit the ASSURED concept perfectly – it is widely available, inexpensive, user-friendly, robust, lightweight, deliverable and sustainable.[12] Further, the nature of paper favors the disposal of contaminated samples, *e.g.* through burning, even without available waste treatment facilities.

Paper-based cell study platforms have been explored in previous studies, utilizing the tunable physical and chemical properties of paper, and its fibrous structure as a scaffold for 3D cell studies.[14,15] Cell cultivation areas on the paper have been manufactured by wax printing,[16] or photolithography.[17] More intricate set-ups include a filter paper strip based set-up with physisorbed cells and a self-contained portable sensing system for detecting semi-quantitative cell quorum sensing of signaling molecules in samples,[18] and a 3D cell culture set-up formed by stacking papers impregnated with suspensions of cells in an extracellular matrix (ECM) hydrogel.[19] Yet another approach to 3D-stacked paper-based culture systems has been manufactured by wax printing a well plate template which was then seeded with valve cell and collagen mixtures[20] and used as a model for cardiac ischemia.[21] Paper-based platforms can also support advanced diagnostic analyses, *e.g.* toehold switch sensors for detecting bacterial toxins[22] or DNA sensors for diagnosing malaria.[23]

The aim of this study was to develop a low-cost sustainable paper-based test platform with improved cytocompatibility and versatility for bioanalytical studies. Here a latex composite coating was introduced on a paper substrate in order to create a liquid barrier and to create a surface with improved cytocompatibility. Indeed, excellent barrier properties against water, ethanol and oil are reported enabling long-term bio-analytical studies using *e.g.* cell media. Most importantly, the composition of the composite coating can be optimized and tuned for improved cell–substrate interactions. A test array was constructed by printing patterns of polydimethylsiloxane (PDMS) or wax onto the latex film. This pattern makes up an assay for multimodal control of cellular processes such as cell proliferation, cell migration and cell viability. Example uses of the platform for cytocompatibility, cell- or materials studies, as well as screening of active pharmaceutical ingredients are demonstrated. We also demonstrate that the data from this platform can be collected and analyzed reliably without the need for expensive instrumentation.

2 Experimental

2.1 Materials

Latex surfaces. Five different aqueous latex dispersions were used in this study: two commercial latices, and three synthesized latices.

The commercial latex dispersions were: a polystyrene (PS) dispersion (HPY83, Trinseo GmbH, CH) with an average particle size of 130 nm and a glass transition temperature of 105 °C as reported by the manufacturer; and a polymerized acrylonitrile butadiene styrene (ABS) copolymer dispersion (HPC26, Trinseo GmbH, CH) with an average particle size of 140 nm and a glass transition temperature (T_g) of 8–10 °C, as reported by the manufacturer. The PS and ABS dispersions had a solids content of 47.9% and 54.5% respectively.

Synthesized latices. The synthesized latices L-01, L-02, and L-05 were prepared *via* a semi-batch emulsion polymerization. The reactions were carried out in a 0.5L reactor equipped with a water heating jacket, a mechanical stirrer, a reflux condenser and two inlet lines. Distilled water was used to prepare the aqueous solutions which were stirred at 200 rpm for the entire duration of the reactions. A pre-emulsion was prepared by mixing acrylic acid, butyl acrylate and styrene (each purchased from Sigma-Aldrich, Finland) and emulsifiers (*i.e.* Disponil FES 32 and Disponyl NG 1080, purchased form BASF) in distilled water for 30 min at room temperature. A mixture containing the anionic surfactant (Calfax DB 45) solution and 50% of the total amount of the initiator (ammonium persulfate) solution was poured into the reactor and heated to 80 °C under stirring. The remaining initiator solution and the pre-emulsion were fed into the reactor through the inlet lines using two peristaltic pumps. The feeding flow was adjusted to feed the solutions in about 2 h. After the feeding phase was completed, the reactor was kept at 80 °C for 2 h in order to ensure the total consumption of monomer residues. The temperature was then lowered to 55 °C, within 20 min, and the redox agents (*tert*-butyl hydroperoxide TBHP and sodium formaldehyde sulfoxylate) were added. The system was allowed to react for an additional 30 min at 55 °C before being cooled to 30 °C. Ammonium hydroxide solution was then added to adjust the pH. The obtained latex was filtered through a 125 μm filter mesh in order to remove eventual coagulum. The solid content of each product was measured. Thermogravimetric analysis were performed using a SDT Q600 and a DSC 250 from TA instruments (Delaware, US). Both measurements were conducted under N_2 atmosphere (flow rate 100 ml min^{-1}) at a heating/cooling rate of 10 °C min^{-1}. The formulations are given in the Table 1 below, with some end product characteristics in Table 2.

PDMS. The used PDMS contained vinyl groups (Dehesive® 920 by Wacker Chemie, AG, Germany) and was synthesized using Wacker Chemie's (Germany) chemicals Wacker® catalyst OL and Crosslinker V24 (mixing ratio 100 : 2.5 : 1 wt%). The PDMS was cured at 80 °C.

Solid ink. The solid ink, hereon referred to as 'wax', was a black Xerox Colorqube 8570 108R00930 ink (Norwalk, CT, USA).

Well plate. Commercial CELLSTAR® (Greiner, USA) well plates were used as a reference substrate. The plates were made of polystyrene and they were provided sterile by active surface treatment.

Cell culture. Human dermal fibroblasts (HDF) and cervical cancer cells (HeLa) were obtained from ATCC (Manassas, VA, USA) and maintained in DMEM medium (Sigma-Aldrich)

This journal is © The Royal Society of Chemistry 2020

J. Mater. Chem. B, 2020, **8**, 1146–1156 | **1147**

Table 1 Composition of the synthesized latices

	L-01 [g]	L-02 [g]	L-05 [g]
Pre-charge			
Water	200	200	200
Calfax DB 45	0.06	0.06	0.06
Initiator			
Water	47	47	47
Ammonium persulfate	1.34	1.34	1.34
Pre-emulsion			
Water	100	100	100
Acrylic Acid	4.30	4.30	4.30
Butyl Acrylate	0	102	0
Styrene	200	98	200
Disponil FES 32	4.61	4.61	3.83
Disponil NG1080	1.16	1.16	1.16
Redox solution 1			
Water	1.70	1.70	1.70
tert-Butyl hydroperoxide	0.20	0.20	0.20
Redox solution 2			
Water	0.90	0.90	0.90
Sodium formaldehyde sulfoxylate	0.17	0.17	0.17
pH adjuster solution			
Water	0.90	0.90	0.90
Ammonium hydroxide	3.00	3.00	3.00

Table 2 Properties of the synthesized latex

	Solids content in dispersion (%)	T_g (°C)	Particle size
L-01	35	100	147 nm (STD 2.3)
L-02	35	16	301.1 nm (STD 5.7)
L-05	35	100	250.8 nm (STD 3.5)

supplemented with 10% foetal calf serum (BioClear, Wiltshire, UK), 2 mM L-glutamin, 100 U ml^{-1} penicillin, 100 μg ml^{-1} streptomycin at 37 °C in a 5% CO_2/95% O_2 and 90% relative humidity atmosphere and maintained under sterile conditions in a cell culture incubator. The cells were passaged three times a week at a 1 : 3 split ratio and used under 20 passages in order to maintain normal fibroblast phenotype.

Base paper. The base paper used in this study was a commercial uncoated paperboard (from here on referred to as BKS) produced by BillerudKorsnäs (Sweden). The board had a basis weight of 272 ± 2 g^{-2} and thickness of 348 ± 3 μm.

Doxorubicin. Doxorubicin (DOX, Sigma-Aldrich), was chosen as the model drug for drug testing on the paper-based platform.

2.2 Methods

IGT Flexographic printer. Patterned PDMS structures were printed using a laboratory scale printability tester (IGT Global Standard Tester 2, IGT Testing Systems, The Netherlands). Printing was done at an ambient temperature of 23 °C and a relative humidity of 50%. The used anilox roll had a cell angle of 45°, a cell volume of 20 ml m^{-2} and a line count of 40 lines per cm. For ink transfer a patterned photopolymer printing plate, produced by Ohkaflex, Espoon Painolaatta, Finland, was used. ''Reaction areas'' or ''wells'' refer from here on to the non-printed areas (*i.e.* areas free of PDMS). The printing speed was set to 0.5 m s^{-1}; the printing pressure between anilox roll and printing plate was set to 100 N, and the force between printing plate and substrate was set to 50 N.

Wax printer. Wax printing was used to create patterned structures on the latex-coated paper substrates. A Xerox ColorQube 8570 (Norwalk, CT, USA) wax printer was used and rows of four circular non-print areas of 7 mm diameter were printed to form the test array (Fig. 3).

Reverse gravure coatings. Latex dispersions were coated onto the substrate papers with a commercial MiniLabo reverse gravure coater (Yasui Seiki Co., Japan). The nanostructured coatings were done with a microgravure roll of 120 lines per inch and a 65 μm depth, giving an approximate wet thickness of 5–11 μm (transfer fraction was 0.28). Coating web speed was 0.5 m min^{-1} and the gravure roll rotational speed 25 rpm. Two 1kW IR driers provided sufficient drying power.

IR heating. The nanostructured surface texture was finalized by irradiating the latex-coating with a short-wavelength infrared (IR) heater (IRT systems, Hedson Technologies AB, Sweden).

Contact angle measurements and surface energy determination. A CAM200 goniometer (KSV Instruments Ltd CAM200, Finland) was used to determine the equilibrium contact angle (θ_a) of three probe liquids: MilliQ water, diiodo methane (DIM) and ethylene glycol (EG). Droplets of 2 μl volume (1.4 μl for diiodo methane) were dispensed on the surface and droplet form was captured for 25 s with a frequency of 4 frames per second for the initial 5 s followed by a capture rate of 1 frame per second for 20 s. The contact angles at each measurement point were determined with software supplied with the instrument, which used a Young-Laplace fitting method to the drop silhouette curvature.

Surface energies were then calculated with the Owens–Wendt–Rabel–Kubelka (OWRK), and van Oss–Chaudhury–Good and Kabel methods, respectively. The used surface tension values were those suggested by van Oss–Chaudhury–Good.

Barrier testing. To assess the barrier properties provided by the latex coatings, a modified experimental setup based on the prism method was used.[24] Briefly, a glass prism was utilized for monitoring the change in the refractive index with time caused by the penetration of the solvent through the sample. Uncoated paperboard was used as a reference. Then the substrate were coated with the PS:ABS latex blend (one or two layers), and tested with three types of solvents: deionized water, ethanol, and vegetable oil. The results were obtained as a time series of images. Initially, the studied area was shown as a black area, but as the liquid penetrated the sample and the effective refractive index changed, the wet areas appeared as white spots. The images obtained from the prism method were analyzed with an open source Java image processing program FijiImageJ and the count of white pixels as a function of time was transformed into a curve illustrating the effective barrier properties.[25,26]

Crystal violet staining for quantifying cell growth. Both HDF and HeLa cells were first seeded on different colored paper strips in an increasing amount of cells per 11 mm diameter ''well'' as an estimation of cell growth. The seeding densities

1148 | *J. Mater. Chem. B*, 2020, **8**, 1146–1156

This journal is © The Royal Society of Chemistry 2020

were as follows: 0, 1×10^3, 3×10^3, 5×10^3, 10×10^3, 15×10^3, 20×10^3, 30×10^3 cells. Cell growth was analyzed after 24 h, 48 h or 72 h and the amount of cell medium used was 100 µl per well. As a comparison, cells were also grown on 48-well plates with a well of 11 mm with the recommended volume of 200 µl minimum amount of cell medium. For staining, the cells were washed with phosphate buffered saline (PBS), and then stained using 0.2% crystal violet in 2% ethanol water solution for 10 min at room temperature. The excess dye was removed with repeated water washing and the samples were dried overnight at room temperature. The stained strips were scanned with an office scanner (*e.g.* CanonScan LiDe 120) at a resolution of 600 dpi. Thereafter, the images of the strips were analyzed using an in-house made analytical software. For analyzing the amount of cells in the multi-well plates, the crystal violet dye was re-solubilized in 2% sodium dodecyl sulphate (SDS) and the absorbance of each well was determined at 570 nm using an Hidex Sense Beta Plus microplate reader (Hidex Oy, Turku, Finland). Statistical analysis was done with GraphPad Prism® 6.0 (San Diego, California, USA).

Atomic force microscopy. Topographical imaging of the surfaces was conducted with Bruker's Nanoscope V MultiMode 8 atomic force microscope (AFM). 5 µm by 5 µm images with a resolution of 1024 by 1024 pixels were captured at a scan speed of 0.391–1.00 lines per second. The used silicon cantilevers had a nominal tip radius of 10 nm (NSG10, NT-MDT, Russia).

The image analysis software Scanning Probe Image Processor (SPIP) by Image Metrology (Denmark), was used for image analysis and calculation of the surface roughness parameter values. The surface coverage fraction of the hard PS component was determined from the height histograms. Filtering of the obtained topographs of the latex surfaces was conducted with the software's Gaussian filter according to ISO 11562 standards. A 0-th degree LMS fit was also applied as necessary.

The roughness parameters were calculated from 5 µm by 5 µm images. The parameters used for quantifying the surfaces were the following: the surface area ratio (S_{dr}), which is a measure of the roughness-induced increase of area compared to the projected flat plane. The RMS roughness (S_q) is the square root of the sum of all height points' difference in z-direction from the mean line, *i.e.* the standard deviation of surface heights. This is a measure of the vertical height variations of the surface. The density of local maxima, summits, is given by the summit density parameter (S_{ds}). The correlation length from the autocorrelation function (S_{cl37}) is a measure of the lateral spacing between surface features, the definition being the length of surface over which the correlation function decays to 37%, *i.e.* $1/e$, of its initial height at origin.[27,28] S_{fd} is the fractal dimension of a surface. Perfectly flat surfaces have a fractal dimension of 2.0, Brownian surfaces have a S_{fd} of 2.5 and a form with a fractal dimension approaching 3 fills space almost like a volume. This characteristic has been indicated to affect cell adhesion.[29]

Inkjet printing of drugs. Drug loading of the wells was conducted as follows: first DOX was dissolved in MilliQ water (0.1 mg ml^{-1}) and the printing solution was injected into a new disposable plastic cartridge (Canon quick-fill) using a sterile syringe through a 0.2 µm polyethersulfone (PES) membrane filter. A number of layers (1–14) of the working solution was inkjet-printed into the wells according to the pre-made design using an Epson XP-760 (Japan) desktop printer. The comparability of the different methods was tested by comparing the effect of dried DOX both in the hydrophobic wells on the paper-platform and in a multi-well plate on HeLa cells, and furthermore by comparing DOX added to the cell medium at similar concentrations. In the dried application method cells were seeded on top of the drug dried on the carrier substrate compared to the in-medium application, where the drug was homogeneously mixed into the cell medium containing the cells. In all cases 30×10^3 cells were seeded per well and incubated for 24 h, after which cells were stained with crystal violet in order to analyze the efficacy of the drug.

Statistical analysis. Statistical significance (*p*-value) was determined by two-way analysis of variance using Sidak's multiple comparisons test (GraphPad Prism® 6.0, San Diego, CA, USA). Error bars in cell data figures represent plus per minus standard error of the mean ($\pm$ SEM), one star symbolizes a significance level of 0.05 ($P \leq 0.05$), two stars the level of 0.01 ($P \leq 0.01$), three stars the level of 0.001 ($P \leq 0.001$), and four stars a significance level of 0.0001 ($P \leq 0.0001$).

3 Results

3.1 Characterization of the paper substrate

The cell study platform was manufactured by coating the paperboard substrate with a 50:50 blend of polystyrene (PS, HPY83) and acrylonitrile butadiene styrene (ABS, HPC26) latices. The intensity of the IR drying was adjusted so that the PS particles were partially annealed and flattened, giving a surface topography with flattened PS spheres evenly distributed over the ABS.[25]

Firstly, the latex coating decreased the roughness of the substrate (topography of uncoated board showed as an example in Fig. 1A). The bimodal latex surface has been previously shown to stimulate cellular proliferation due to a combination of nanoscale surface roughness and surface chemistry.[23] The bimodal structure with a specific height profile is a result of the combined effect of the two latex components, the hydrophobic high-T_g PS remaining as particles even after annealing and the hydrophilic low-T_g film-forming ABS (Fig. 1B). In addition, the stiffnesses of the two components in a blend coating of commercial latices have been previously determined as 0.13 GPa for ABS and 1.61 GPa for PS.[30]

Correspondingly, the board was coated with 70 : 30 blends of L-01 and L-02 (Fig. 1C), as well as L-05 and L-02 (Fig. 1D). As shown in Fig. 1 these coatings give a distinct surface morphology compared to the commercial blend.

An array of planar spherical cell culture wells were created by flexographic printing of a pattern of PDMS on top of latex-coated substrates. The pattern consisted of 8 mm in diameter circular areas free of PDMS. Alternatively, a printed wax pattern similar to the PDMS pattern was deposited onto the surfaces.
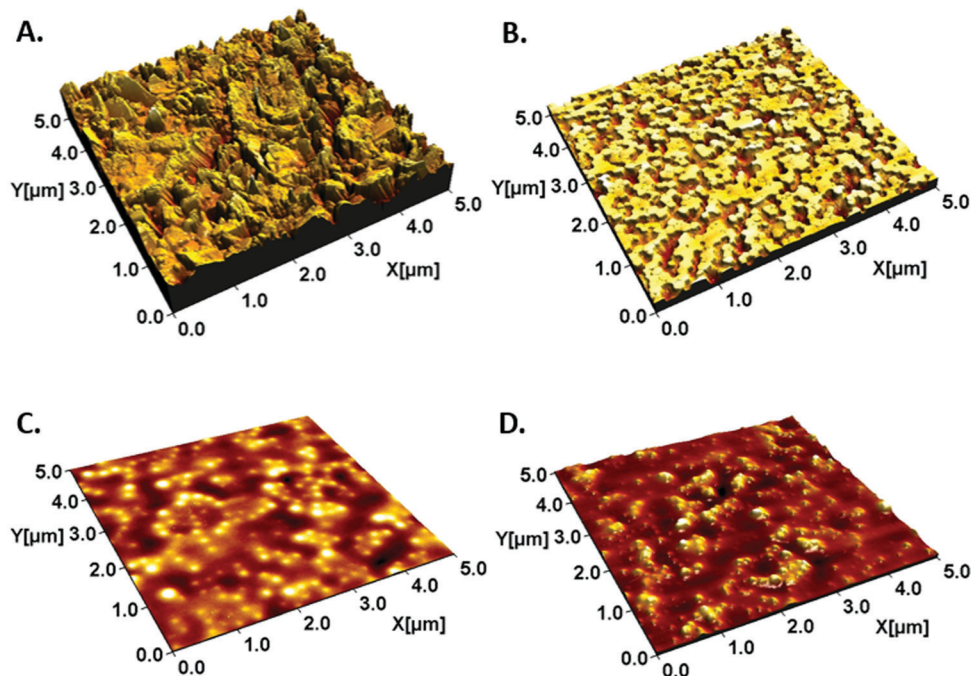
This journal is © The Royal Society of Chemistry 2020

J. Mater. Chem. B, 2020, **8**, 1146–1156 | **1149**

Fig. 1 AFM images of the surfaces used in the study. All images are of 5 μm × 5 μm size, with the height scales exaggerated by a factor of 2 for illustrative purposes. (A) The used paper board substrate (image height span of 632 nm); (B) the commercial latex blend of PS:ABS (image height span of 153 nm), (C) the synthesized latex blend L-05:L-02 (image height span of 29 nm); (D) the synthesized latex blend L-01:L-02 (image height span of 93 nm).

In both cases the hydrophobic PDMS or wax limited the wetting to the circular areas free of PDMS, forming an array of circular regions of interest (ROI) where cell culture could be performed.

Contact angles and the respective surface energies calculated therefrom are collected in Table 3. Paper substrates coated with both the commercial latex blend and the two synthesized latex blends showed similar wetting – the water contact angle was 77° for the HPY83:HPC26 coating and 73° for both the L-01:L-02 and the L-05:L-02 coatings. The synthesized polymer blend surfaces were similar to each other in surface chemistry as well as wetting, with a total surface energy of about 38 mJ m^{-2}, with a polar component of 9.8 mJ m^{-2}. The commercial blend was slightly more energetic with a total surface energy of

ca 39 mJ m^{-2}, and a polar contribution of 6.8 mJ m^{-2}. The surface energy of the ColorQube wax was lower, 29.0 mJ m^{-2}, with dispersive contributions only. The water contact angle on wax was 109°. The hydrophobic PDMS (water contact angle 114°) used for forming the well structures had in turn a very low surface energy, 12.4 mJ m^{-2}. There was also a small difference between the polar components of the surface energy of PDMS and the wax: PDMS had a very low polar component at 0.6 mJ m^{-2} whilst the wax had a negligible polar component of 0 mJ m^{-2}.

Analysis of surface energetics is important since surface chemistry affects interactions of proteins and cells with the substrate. For instance, the electron donor properties have been shown to directly affect the cell–material interaction of HDF cells, while the total surface free energy and relative contributions of the components affects the protein adsorption-mediated cell–surface interactions.[31,32]

The roughness parameters for the surfaces are shown in Table 4, with additional data in the ESI.† The coatings had greater differences in terms of surface roughness and topography

Table 3 Contact angle data, corrected for roughness, and the corresponding calculated determined with the OWRK method for the different substrates polydimethyl siloxane (PDMS), wax, the paperboard (BKS), the commercial latex blend (HPY83:HPC26) and the synthesized latex blends L01-L01 and L05-L02. Surface tension values for the probe liquids water, ethylene glycol (EG) and diiodo methane (DIM) were as suggested by van Oss, Chaudhury and Good. The contact angle values include the standard deviation

Sample	Contact angle [°]			Surface energy [mJ m^{-2}]		
	Water	EG	DIM	Dispersive	Polar	Total
PDMS	114 ± 1	92 ± 2	96 ± 1	11.8	0.6	12.4
ColorQube Wax (black)	109 ± 1	85 ± 1	59 ± 1	29	0.0	29.0
BKS	65 ± 2	64 ± 1	71 ± 4	22.3	17.3	39.6
HPY83:HPC26	77 ± 3	50 ± 3	53 ± 2	32.6	6.3	38.9
L01-L02	73 ± 1	73 ± 1	61 ± 3	28.0	9.8	37.8
L05-L02	73 ± 2	76 ± 1	61 ± 3	28.0	9.8	37.8

Table 4 Surface roughness data with standard deviations determined from 5 μm x 5 μm AFM images for the surface coatings used in cell studies and the supporting base paperboard. Used parameters are RMS-roughness (S_q), effective surface area (S_{dr}) and the fractal dimension (S_{fd})

	S_q [nm]	S_{dr} [%]	S_{fd} [−]
BKS	52.8 ± 7.6	85.9 ± 16.6	2.18 ± 0.03
HPY83:HPC26 50:50	23.0 ± 0.2	24.7 ± 0.9	2.22 ± 0.02
L01–L02 70 : 30	13.2 ± 0.2	1.9 ± 0.1	2.02 ± 0.03
L05–L02 70 : 30	3.3 ± 0.1	0.3 ± 0.01	2.19 ± 0.01

1150 | J. Mater. Chem. B, 2020, 8, 1146–1156

This journal is © The Royal Society of Chemistry 2020

than in terms of wetting and surface energies. The PS:ABS coating had a bimodal surface structure consisting of high PS regions and intermittent valleys of ABS. The PS:ABS coating had the highest roughness among the studied coatings, with an RMS roughness (S_q) of 23 nm, and an effective surface area (S_{dr}) of 25%. Interestingly, this surface also had a fractal dimension, S_{fd}, of 2.22 that was closest to that of a Brownian geometry (S_{fd} = 2.5) of all the coated substrates studied.

The surface films of the synthesized latices, the blends of L01 and L02 as well as L05 and L02, on paperboard were smoother and had a very different topography compared to the surfaces made from the blend of commercial latices. Of these two the L01–L02 blend had an S_{dr} of 1.9% and an S_q of 13.2 nm, appearing rougher than L05–L02. The fractal dimensions of these surfaces, S_{fd}, were 2.02 for the L01–L02, and 2.19 for L05–L02.

The cell–material interface offers a means to passively control the attachment of cells. For instance a moderately smooth surface in terms of the parameters S_q, S_{dr} and normalized roughness has been found to be preferential for high HDF proliferation.[29,30] Also, topologies with a Brownian fractal dimension 2.5 have been speculated to activate the FAK signaling pathway, and through that mechanism increase cell proliferation.[29,33] For applications or studies that are used with specific cell lines this tuning can be done more freely, as different cell types can react very differently to different surface properties.[29]

3.2 Barrier tests

For the purpose of cell studies, the carrying substrate must show sufficient barrier properties to the cell media and other liquids used during cell testing. The barrier must also be retained over the time needed to perform an experiment, typically 24–72 h. In our platform, the PS:ABS polymer blend coating provided the barrier intrinsically, as confirmed by prism type barrier tests. After optimization, the barrier properties gave full retention of liquids for several days, allowing long-term cell studies.

Fig. 2 shows the time each sample remains a 90% barrier for the test liquids (deionized water, ethanol and vegetable oil). The value 90% corresponds to 10% of the analysed pixels showing signs of liquid penetration. The uncoated commercial board had poor barrier properties against all solvents, the barrier percentage reaching 90% in less than 50 min for deionized water, 2 s (approx. 0.03 min) for ethanol, and 22 s (approx. 0.37 min) for vegetable oil.

One layer of coating of the commercial latex blend was sufficient to generate a barrier for deionized water for the duration of the experiment, but not for ethanol and vegetable oil, where two layers of the latex coating was required for a proper barrier for the full 72 h. One layer of coating was therefore only enough when the base substrate already possessed good barrier properties. Defects on the coating layer, such as pinholes, or irregularities in the base substrate itself allow for penetration of the solvent into the sample. Consequently, two layers of coating of the latex blend is to be recommended as the best design to prevent the penetration of all the solvents during up to three days of exposure.

3.3 Cell studies using the platform

The applicability of the paper-based platform for *in vitro* cell culture studies was demonstrated with a seeding density experiment. An increasing number of HeLa and HDF cells were seeded into the wells as shown in Fig. 3. The predetermined seeding densities were pipetted into the wells after the paper substrates had been washed with ethanol and MilliQ. Then the wells were topped-up with DMEM cell media to a total volume of 100 µl. As a comparative reference, glass cover slips coated with the latex blend and placed in a conventional well were used. The paper substrates and well plate were kept in an incubator under controlled conditions for the given duration (24–72 h).

After the given proliferation time, both cell cultures were stained using crystal violet (CV). The method stains viable adherent cells thus detecting differences in cell growth as an end point measurement (Fig. 4). The read-out from the multi-well plate
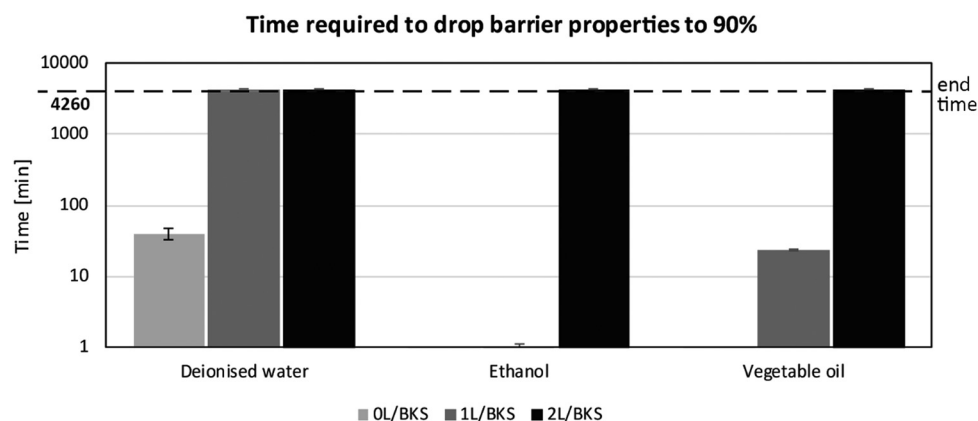
Fig. 2 Time required to lose successful barrier properties. The substrates tested were BKS with an increasing number of coating layers: uncoated (0L), one layer of latex coating (1L), or two layers of latex coating (2L). The threshold set for defining sustained barrier properties was 90%, indicating a significant penetration of the solvent into the sample under that value. The maximum tested time of interaction (dashed line) was 4260 min (3 days) with the solvents deionised water, ethanol, and vegetable oil. The data represented is the average of three replicates with standard deviations.
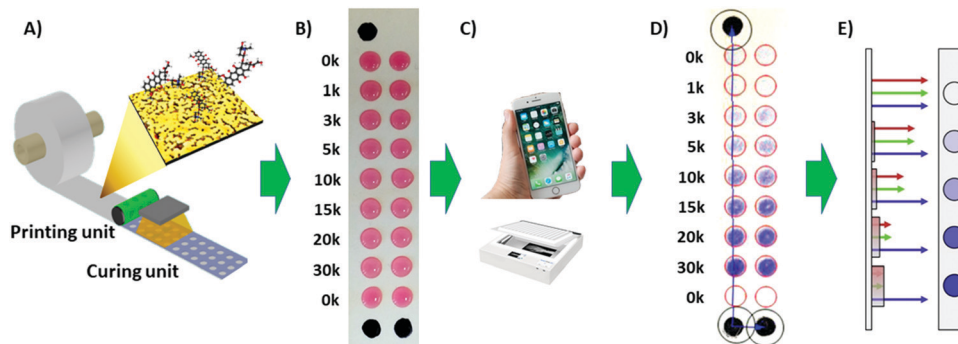
This journal is © The Royal Society of Chemistry 2020

J. Mater. Chem. B, 2020, **8**, 1146–1156 | **1151**

Fig. 3 A concept scheme for the developed platform. (A) The base paper is first coated with a nanostructured barrier coating, and materials of interest, such as doxorubicin as illustrated, are then deposited in the well structures formed by *e.g.* hydrophobic polydimethylsiloxane (PDMS). (B) Cell culture is then performed on the wells, and the cells stained. (C) The paper strips are captured with office scanners or smart phone, and (D) the images analysed using a software for colour variations that can be analysed for the cell response in each well, (E).

was done with a commercial plate reader analyzing the absorbance at 570 nm wavelength. The read-out of the paper-based screening platform was based on the color intensities, in RGB form, of the wells and was analyzed from their images obtained with an office scanner. The analysis was done using a custom-made software, which is able to identify and detect the well geometry and subsequently analyze the color of each well, the intensity being proportional to the amount of CV-stained DNA present in the well. This by extension corresponds to the amount of cells present in the well or wells studied. A full description of the software and the analysis method can be found in ESI.†

Data from both the HDF and HeLa cell viability assay is summarized in Fig. 4. The data indicates comparable performance between the two methods as can be seen from the comparable error in both studies. The conventional well plates are ill suited to testing *e.g.* the biocompatibility of novel materials because of the difficulty to process the bottom of the well plate by *e.g.* coating. In contrast, the paper-based platform opens up many possibilities for biomaterials testing through easy functionalization of the surface by *e.g.* printing, coating or self-assembly. Another benefit of using coated paper is minimal background staining for control and low seeding densities (30×10^3), whereas a coffee ring effect of staining

agent (CV) around the edges of the coated coverslips in the multi-well plate can give a false positive readout when using a standard plate reader. This can be seen as a rather high read-out for 0×10^3 seeded HDF cells in Fig. 4. Using the nanostructured polymeric coating that enhances cell proliferation[30] on the paper substrate allowed the detection of clear differences in cell numbers in a shorter time. Incubation times longer than 72 h would require changing the cell media on a paper-based platform due to evaporation of the low volume (100 µl) of cell media used (data not shown).

3.4 Cytocompatibility studies

To further illustrate the versatility of the paper based platform for material testing the capability for cytocompatibility studies was tested. For this purpose latex blends, denoted L-01:L-02 and L-05:L-02 (see 'Materials' section) were rod-coated onto the paper board and IR-dried similarly as the commercial latex coatings. The PDMS pattern of planar 8 mm circular wells that formed the cell culture areas were flexographically printed onto the latex-coated paper. 0, 1×10^3, 10×10^3, 20×10^3, and 30×10^3 of HDF and HeLa cells were seeded into the wells for 48 h in order to estimate the cell viability on the latex blends. The analysis of the cell numbers on the paper strips was conducted as described earlier. The results are presented in Fig. 5.
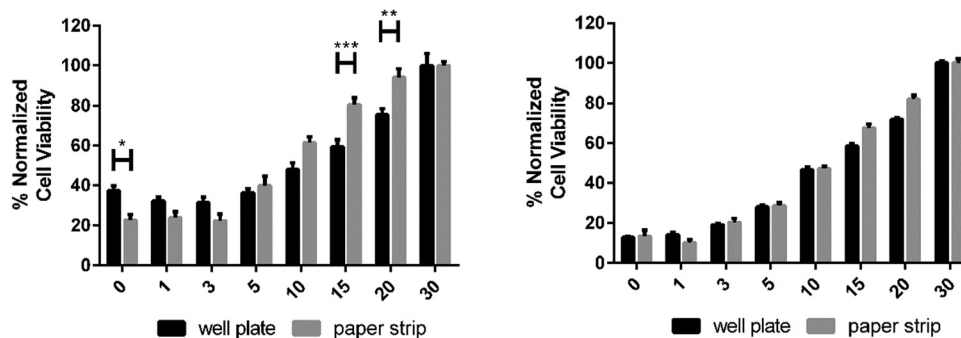

Fig. 4 A comparison of basic cell viability assays using both the SE paperboard strips coated with a 50:50 blend of HPY83:HPC26 (PS:ABS) and a well plate, with an increasing amount of seeded cells (in 10^4) using HDF (left) and HeLa cells (right). In both cases the maximum readout has been normalized to each method's highest cell count – 30×10^3 of seeded cells. The data presented are averages of 4 repetitions ($n = 4$). Cells were cultured over 24 h.
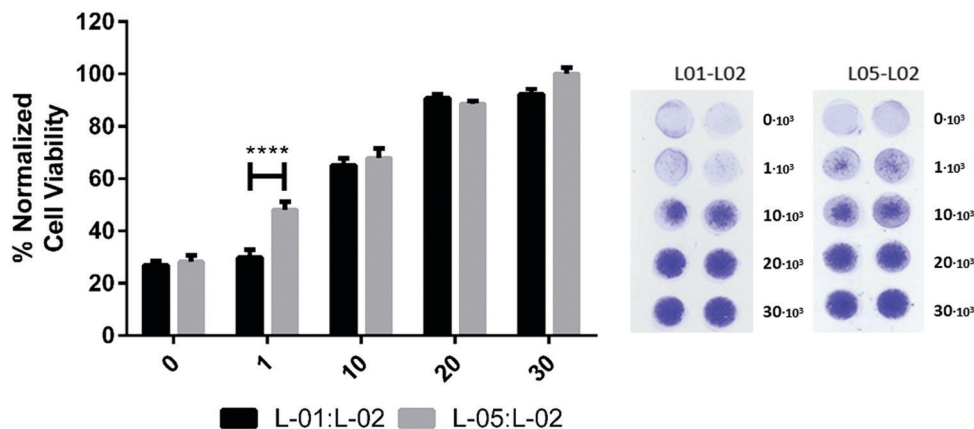
Fig. 5   Color intensity readout (left) of an increasing amount of seeded HeLa cells on two types of coatings on paper, L-01:L-02 and L-05:L-02, with representative images of the analyzed paper strips after CV staining (right). Note that the bar chart data has been normalized towards the L-05:L-02 30×10^3 wells with the largest color intensity.

For both blends L-01:L-02 and L-05:L-02, the wells seeded with 30×10^3 cells were observed to be largely covered by the CV stain. This indicated the presence of cell colonies all over the well area, and a high degree of cytocompatibility. Although affinity of the crystal violet stain to the surface was seen as a background level readout (0×10^3 data) the color intensity in the wells increased clearly with a growing amount of seeded cells for both latex blends. When comparing the trends of the color intensity readouts *versus* the seeded cell amount for the two surface coatings, differences in the cellular viability between the coatings were discerned.

The color intensity readout, *i.e.* the number of cells, from the L-05:L-02 blends increased linearly with an increasing amount of cells seeded in the wells. In all wells some colonies were visible – the largest seeding amounts clearly covering most of the available well area. In the case of the L-01:L-02 blend, a seeding amount of 1×10^3 could not support a cell culture, as indicated by a color intensity on the level of the blank. Only a scarce few were visible in the wells. At 10×10^3 and 20×10^3 densities the cells thrived almost as well as on the L-05:L-02 coating. The 20×10^3 cell count also appeared, both visually and with the stochastic color analysis, to differ less from the 30×10^3 seeded wells than expected. This could be interpreted as the maximum number of supported cells plateauing at the level, or cells beginning to grow on top of each other. Overall, the maximum number of sustained cells was observed to be less than on the L-05:L-02 counterpart. This is interpreted as the cells spreading and proliferating well enough on the surface to cover most of it during the 24 h growth period, limited by the chemical and topographical properties of the coating.

3.5   Paper-based platform for drug screening

Doxorubicin (DOX) specifically kills cancerous cells while leaving normal cells unharmed. It also has both a visible color as well as fluorescent properties, making this drug a suitable candidate for estimating the usability of the paper-based platform for drug screening.

The testing was designed to compare varying amounts of DOX deposited both on cover slips in a well plate and on the paper-based platform; in the prior case being deposited by pipetting and in the latter case either pipetted or inkjet-printed into wells of the paper-platform. 30×10^3 HeLa cells were then seeded into the wells of both systems, after which the cell numbers were analyzed after 24 h, using the CV staining method and the analysis software described previously for the paper-based study antagonistically to the commercial well plate software.

In order to determine the amount of DOX loaded into the wells by inkjet-printing, a standard curve was prepared (see ESI†). This allowed for comparing the amount of drug dissolved into PBS from DOX inkjet-printed into the wells to a known loading by pipetting, *i.e.* the standard. As the inkjetted layers of DOX dried before the drug dissolution study the standard done by pipetting was also dried before dissolution into PBS for best comparison between the methods. From the standard curve it was read that 6 layers of inkjet-printed DOX gave a concentration of *ca*. 0.5 µg ml^{-1} and that 13 layers was roughly equivalent to 1.0 µg ml^{-1}. AFM images of the well loaded with 7 layers of DOX (see Fig. 6) show the disposed droplets forming discrete regions of the drug over the nanostructured topography of the commercial latex blend coating.

The plate reader data showed a reduced HeLa cell viability with DOX concentrations above 0.25 µg ml^{-1} (Fig. 6). In both studies the paper strips showed a strong reduction of cell viability with doses larger than 0.25 µg ml^{-1}. These two studies showed a further 50% reduction in viability between 0.25 µg ml^{-1} and 0.50 µg ml^{-1}; the cell viability was reduced more slowly in the well plate study being reduced by *circa* 25% from 0.25 µg ml^{-1} to 0.50 µg ml^{-1} (Fig. 6 and 7). Meanwhile, the reduction of HDF cell viability was relatively minor compared to HeLa cells. At the presence of DOX the viability was reduced by *circa* 20–25% at concentrations ranging from 0.01 µg ml^{-1} to 0.5 µg ml^{-1}. At higher concentrations the viability decreased further to *circa* 60%, which is still clearly higher than the viability of HeLa cells at similar DOX concentrations. The viability of HDF cells, however, remained above 50% even when using the highest concentration of DOX (5.0 µg ml^{-1}). These HDF are considered non-cancerous and are therefore not as susceptible to the toxic effect of doxorubicin in the used concentrations.[34]
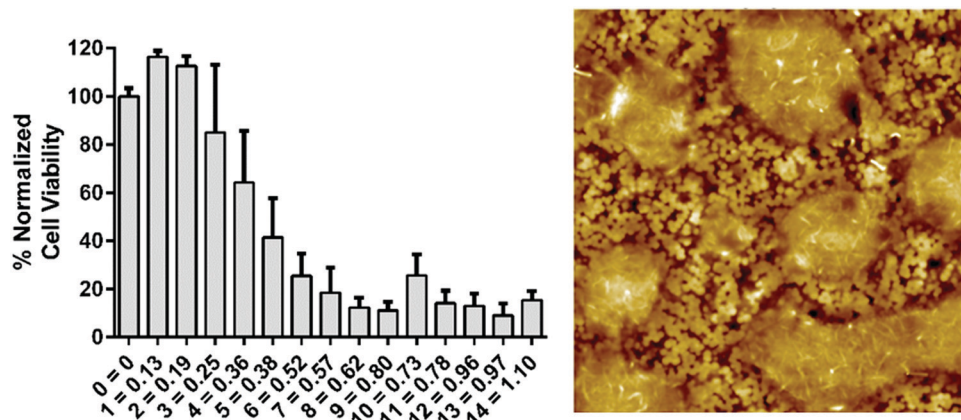
Fig. 6 (left) The viability response of HeLa cells to an increasing amount of doxorubicin deposited by inkjet printing. The bar labels are given as layers of drugs printed with estimated drug concentration in $\mu g\ ml^{-1}$. (right) An AFM image of 10 μm × 10 μm size of a well with 7 inkjet-printed layers of doxorubicin solution.
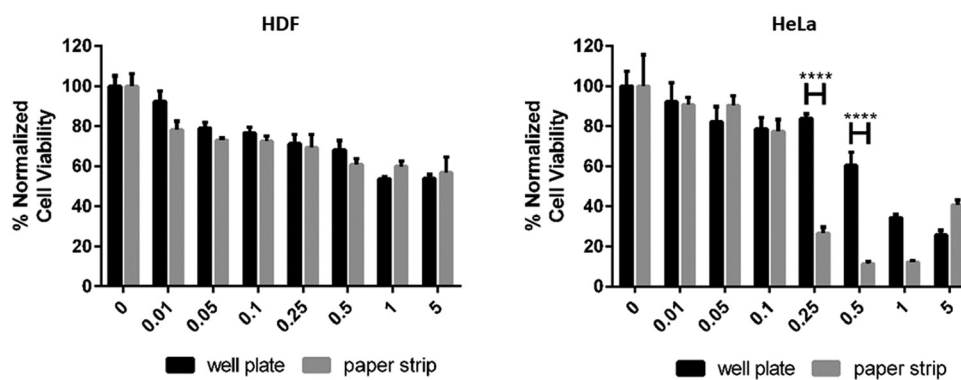

Fig. 7 The viability response of HDF (left) and HeLa cells (right) to an increasing amount of doxorubicin in $\mu g\ ml^{-1}$, pipetted into the wells of a well plate (plate reader data) and a paper strip.

Comparable data were obtained from the HeLa cell viability studies in Fig. 7 from the inkjet-printed viability studies seen in Fig. 6. This corresponds to previously published data showing a sharp reduction of cell viability of HeLa cells when exposed to 0.1–5.0 $\mu g\ ml^{-1}$ concentrations of DOX (in ref. as: adriamycin).[35,36] This demonstrated that a simple affordable experimental set-up, with a tunable coating to fit the experiments' needs, can rival one performed with expensive equipment, in this case the plate reader, for estimating drug efficacy in terms of cell viability using both cancerous and non-cancerous cell lines. All surface modifications demonstrated in these studies are up-scalable, including the application of an active pharmaceutical ingredient (DOX). This has the added benefit of producing highly controllable automated inkjet printing of tailorable drug doses, effectively minimizing human error. A colorimetric read-out is also user friendly, virtually confirming that this paper-based platform conforms to the criteria for being "ASSURED".

4. Discussion

Successful use of a paper-based *in vitro* cell growth platform could challenge the traditional plastic multi-well plate and be one step of downshifting the use of plastic. 2D cell culture,

despite its limitations, still provides a means for quick and easy initial screening and/or preliminary analysis. The paper-based cell growth platform described here can cost-effectively and easily be designed and produced with any planar geometry. It can also be disposable by the nature of paper itself. In addition, the surface of paper (or the latex coating on it) can be further functionalized with coatings, provided that stable barrier properties are obtained through a (pre-)coating. A potential area of application is bio-functionalization, *e.g.* anti-bodies for screening of diseases, or electronics for diagnostics and external stimulation. Autofluorescence of coatings and the base paper also requires forethought when choosing fluorescent dyes.

5. Conclusions

In this work we showed that a stand-alone paper-based cell study platform made from affordable materials suitable for mass production is suitable for cell culture and screening, and can challenge traditional multi-well plates. This was demonstrated through comparing the viability of human cells grown on the paper-based platform with cells grown in conventional plastic multi-well plates. Furthermore, it was demonstrated that paper-based platforms can be made highly tunable in

1154 | *J. Mater. Chem. B*, 2020, **8**, 1146–1156

This journal is © The Royal Society of Chemistry 2020

terms of materials used, and can also be adapted to a number of applications, including basic cell studies, cytocompatibility, drug development and efficacy testing. Another benefit of the paper-based platform compared to a multi-well plate is that it has no geometrical limitations. One of the greatest benefits of using the platform comes from the possibility for versatile surface modifications, *i.e.* functionalization. These could be coatings which can be applied onto the base substrate by large scale processing, such as coating, flexographic printing or inkjetting, providing tunable changes to the surface chemistry and topography in general, but more specifically also the introduction of *e.g.* specific binding sites for analytes of interest or electrodes for sensing or control of cellular processes. Besides these passive properties, active control and stimulus can also be possible by introducing printed electronics to the platform. In this study the paper coating used was intended to enhance the proliferation yield of the used cell lines through its topography, and thus get larger measurable differences in cell numbers during the investigations. The use of the platform for investigating new materials of interest for use in bio-applications was also shown. Indeed, tuning the physico-chemical properties of the materials used, *e.g.* surface chemistry and topography, provides means to passively regulate cellular responses, thus opening a new toolbox in material–cell interaction studies.

Conflicts of interest

There are no conflicts to declare.

Acknowledgements

References

1 M. J. Lerman, J. Lembong, S. Muramoto, G. Gillen and J. Fisher, The Evolution of Polystyrene as a Cell Culture Material, *Tissue Eng., Part B*, 2018, **5**(24), 359–372.

2 M. Oheim, High-throughput microscopy must reinvent the microscope rather than speed up its functions, *Br. J. Pharmacol.*, 2007, **1**(152), 1–4.

3 P. Kankaanpää, L. Paavolainen, S. Tiitta, M. Karjalainen, J. Päivärinne, J. Nieminen, V. Marjomäki, J. Heino and D. J. White, BioImageXD: an open, general-purpose and high-throughput image-processing platform, *Nat. Methods*, 2012, **7**(9), 683–689.

4 S. Tojkander, G. Gateva and P. Lappalainen, Actin stress fibers – assembly, dynamics and biological roles, *J. Cell Sci.*, 2012, **125**, 1855–1864.

5 J. Lee, M. J. Cuddihy and N. A. Kotov, Three-dimensional cell culture matrices: state of the art, *Tissue Eng., Part B*, 2008, **1**(14), 61–86.

6 Y. Tokiwa, P. B. Calabia, C. U. Ugwu and S. Aiba, Biodegradability of plastics, *Int. J. Mol. Sci.*, 2009, **9**(10), 3722–3742.

7 D. Discher, P. Jamney and Y. Wang, Tissue Cells Feel and Respond to the Stiffness of Their Substrate, *Science*, 2005, **310**(5751), 1139.

8 A. J. Rice, E. Cortes, D. Lachowski, B. C. H. Cheung, S. A. Karim, J. P. Morton and A. del Rio Hernández, Matrix stiffness induces epithelial-mesenchymal transition and promotes chemoresistance in pancreatic cancer cells, *Oncogenesis*, 2017, **7**(6), e352.

9 P. A. Jensen, B. V. Dougheryt, T. J. Moutinho Jr and J. A. Papin, Miniaturized plate readers for low-cost, high-throughput phenotypic screening, *J. Lab. Autom.*, 2015, **1**(20), 51–55.

10 R. McNerney, Diagnostics for Developing Countries, *Diagnostics*, 2015, **5**, 200–2009.

11 C. A. Petti, C. R. Polage, T. C. Quinn, A. R. Ronald and M. A. Sande, Laboratory Medicine in Africa: A Barrier to Effective Health Care, *Clin. Infect. Dis.*, 2006, **3**(42), 377–382.

12 A. W. Martinez, S. Phillips and G. Whitesides, Diagnostics for the Developing World: Microfluidic Paper-Based Analytical Devices, *Anal. Chem.*, 2010, **1**(82), 3–10.

13 TechCrunch, 6.1B Smartphone Users Globally By 2020, Overtaking Basic Fixed Phone Subscriptions, 29/05/2017. [Online]. Available: https://techcrunch.com/2015/06/02/6-1b-smartphone-users-globally-by-2020-overtaking-basic-fixed-phone-subscriptions/.

14 K. Ng, B. Gao, K. W. Yong, Y. Li, M. Shi, X. Zhao, Z. Li, X.-H. Zhang, B. Pingguan-Murphy, H. Yang and F. Xu, Paper-based cell culture platform and its emerging biomedical applications, *Mater. Today*, 2017, **20**(1), 32–44.

15 X. Wu, S. Suvarnapathaki, K. Walsh and G. Camci-Unai, Paper as a scaffold for cell cultures: Teaching an old material new tricks, *MRS Commun.*, 2018, **8**(1), 1–14.

16 T. Mazzu-Nascimento, P. A. Gomes Carneiro Leão, J. R. Catai, G. G. Morbioli and E. Carrilho, Towards low-cost bioanalytical tools for sarcosine assays for diagnostics, *Anal. Methods*, 2016, **8**, 7312.

17 E. Carrilho, S. T. Phillips, S. J. Vella, A. W. Martinez and G. M. Whitesides, Paper Microzone Plates, *Anal. Chem.*, 2009, **81**, 5990–5998.

18 A. Struss, P. Pasini, C. M. Ensor, N. Raut and S. Daunert, Paper Strip Whole Cell Biosensors: A Portable Test for the Semiquantitative Detection of Bacterial Quorum Signaling Molecules, *Anal. Chem.*, 2010, **82**, 4457–4463.

19 R. Derda, A. Laromaine, A. Mammoto, S. K. Tang, T. Mammoto, D. E. Ingber and G. M. Whitesides, Paper-suppported 3D cell culture for tissue-based bioassays, *Proc. Natl. Acad. Sci. U. S. A.*, 2009, **106**(44), 18457–18462.

20 M. C. Sapp, H. J. Fares, A. C. Estrada and K. J. Grande-Allen, Multilayer three-dimensional filter paper constructs for the culture and analysis of aortic valvular interstitial cells, *Acta Biomater.*, 2015, **13**, 199–206.

21 B. Mosadegh, B. Dabiri, M. Lockett, R. Derda, P. Campbell, K. Parker and G. Whitesides, Three-dimensional model for

This journal is © The Royal Society of Chemistry 2020

J. Mater. Chem. B, 2020, **8**, 1146–1156 | **1155**

cardiac ischemia, *Adv. Healthcare Mater.*, 2014, **3**(7), 1036–1043.

22 M. K. Takahashi, X. Tan, A. J. Dy, D. Braff, R. Akana, Y. Furuta, N. Dongthia, A. Ananthakrishnan and J. J. Collins, A low-cost paper-base synthethic biology platform for analysing gut microbiota and host biomarkers, *Nat. Commun.*, 2018, **9**(1), 3347.

23 J. Reboud, G. Xu, A. Garrett, M. Adriko, Z. Yang, E. Tukahebwa, C. Rowell and J. Cooper, Paper-based microfluidics for DNA diagnostics of malaria in low resource underserved rural communities, *Proc. Natl. Acad. Sci. U. S. A.*, 2018, **116**(11), 4834–4842.

24 R. Bollström, J. J. Saarinen, J. Räty and M. Toivakka, Measuring solvent barrier properties of paper, *Meas. Sci. Technol.*, 2012, **23**(1), 015601.

25 J. Schindelin, I. Arganda-Carreras and E. Frise, Fiji: an open-source platform for biological-image analysis, *Nat. Methods*, 2012, **9**(7), 671–675.

26 J. Schindelin, C. Rueden and C. M. Hiner, The ImageJ ecosystem: An open platform for biomedical image analysis, *Mol. Reprod. Dev.*, 2015, **82**(7–8), 518–529.

27 J. Järnström, P. Ihalainen, K. Backfolk and J. Peltonen, Roughness of pigment coatings and its influence on gloss, *Appl. Surf. Sci.*, 2008, **254**, 5741–5749.

28 D. J. Whitehouse, *Handbook of Surface and Nanometrology*, CRC Press, Coventry, UK, 2nd edn, 2011.

29 Y. Li, Y. Xiao and C. Liu, The Horizon of Materiobiology: A Perspective on Material-Guided Cell Behaviors and Tissue Engineering, *Chem. Rev.*, 2017, **117**, 4376–4421.

30 E. Rosqvist, E. Niemelä, A. Venu, R. Kummala, P. Ihalainen, M. Toivakka, J. Eriksson and J. Peltonen, Human dermal fibroblast proliferation controlled by surface roughness of two-component nanostructured latex polymer coatings, *Colloids Surf., B*, 2019, **174**, 136–144.

31 H. Juvonen, A. Määttänen, P. Laurén, P. Ihalainen, A. Urtti, M. Yliperttula and J. Peltonen, Biocompatibility of printed paper-based arrays for 2-D cell cultures, *Acta Biomater.*, 2013, **9**, 6704–6710.

32 C. Satriano, S. Carnazza, S. Guglielmino and G. Marletta, Surface free energy and cell attachment onto ion-beam irradiated polymer surfaces, *Nucl. Instrum. Methods Phys. Res., Sect. B*, 2003, **208**, 287–293.

33 C. J. Oates, W. Wen and D. H. Hamilton, Role of Titanium Surface Topography and Surface Wettability on Focal Adhesion Kinase Mediated Signaling in Fibroblasts, *Materials*, 2011, **4**(5), 893–907.

34 T. Sasaki, K. C. Holeyfield and J. Uitto, Doxorubicin-induced inhibition of prolyl hydroxylation during collagen biosynthesis in human skin fibroblast cultures. Relevance to imparied wound healing, *J. Clin. Invest.*, 1987, **6**(1735–1741), 80.

35 S. H. Kim and J. H. Kim, Lethal Effect of Adriamycin on the Division Cycle of HeLa Cells, *Cancer Res.*, 1972, **32**, 323–325.

36 N.-T. Chen, C.-Y. Wu, C.-Y. Chung, Y. Hwu, S.-H. Cheng, C.-Y. Mou and L.-W. Lo, Probing the Dynamics of Doxorubicin-DNA Intercalation during the Initial Activation of Apoptosis by Fluorescence Lifetime Imaging Microscopy (FLIM), *PLoS One*, 2012, 7(9), e44947.

1156 | *J. Mater. Chem. B*, 2020, **8**, 1146–1156

This journal is © The Royal Society of Chemistry 2020